# A Free Interface CMS Technique to the Resolution of Coupled Problem Involving Porous Materials, Application to a Monodimensional Problem

Olivier Dazel, Bruno Brouard, Nicolas Dauchez, Alan Geslain, Claude-Henri Lamarque

# A Free Interface CMS Technique to the Resolution of Coupled Problem Involving Porous Materials, Application to a Monodimensional Problem

Olivier Dazel[1)], Bruno Brouard[1)], Nicolas Dauchez[2)], Alan Geslain[1)], Claude-Henri Lamarque[3)]

[1)] Laboratoire d'Acoustique de l'Université du Maine - UMR CNRS 6613, Avenue Olivier Messiaen, 72 085 Le Mans Cedex, France. olivier.dazel@univ-lemans.fr

[2)] SUPMECA Paris, LISMMA Vibroacoustique, 3 rue Fernand Hainaut, 93407 St. Ouen Cedex, France

[3)] Ecole Nationale des Travaux Publics de l'Etat, DGCB-LGM FRE CNRS 3237, rue Maurice Audin, 69120 Vaulx-en-Velin, France

**Summary**

This paper proposes a Component Mode Synthesis technique for the resolution of problems involving coupled substructures including porous materials. This technique is based on normal modes. A modal subfamily is se-lected for each substructure. Attachment modes are added in order to take into account the influence of non preserved modes. These attachment modes concern both the interface between substructures through interaction forces as well as the external excitation on substructures. A simple criterion based on the evaluation of a residual vector is proposed and allows an automatic selection of the number of preserved modes.

The method is compared to an analytical model in the case of two 1D configurations. The ability of the method to handle coupled systems is shown. The proposed approach perfectly matches with the analytical solution.

## 1. Introduction

### 1.1. Context

Porous materials are heterogeneous media made up of a porous elastic skeleton saturated by a fluid. Assembled structures including porous materials are commonly used in many engineering applications in order to dissipate acoustical or mechanical energy (sound absorption, sound insulation, damping) [1, 2, 3]. In these structures, damping is often due to the inner dissipation mechanisms of the porous material and the optimization of noise control solutions based on the use of such materials requires the development of robust predicting tools.

The dynamical behaviour of porous structures is classically obtained from homogenized models and particularly Biot-Allard's theory [4, 5, 6, 1] which is based on continuous fields mechanics approach. The homogenized porous media is modeled as the superposition of two continuous fields whose inertial and constitutive coefficients are given by phenomenological relations. In many industrial and physical cases, the response of an aggregate structure including porous media to external forces cannot be obtained analytically and it is necessary to use numerical methods to solve the problem. Finite element method is then often used to discretize the poroelastic variational formulation [7, 8, 9, 10, 11, 12, 13]. All of these formulations consider the solid displacement $\mathbf{u}^s$ as unknown of the problem and they differ by the choice of the second field. Some of them [7, 8, 9, 10, 13] (also called displacement formulations) consider an other displacement (fluid, relative flow, total displacement) thereby leading to a 6 degrees of freedom ($dof$) problem; other ones [11, 12] (called mixed formulations) propose to use the interstitial pressure $P$ and correspond to a 4 $dof$ per node problem. However, these numerical models lead to large size linear systems (frequency dependent and complex valued). The development of adapted techniques which can reduce the computational cost of the problem to be solved is then of the utmost importance. Different solutions have still been investigated [14, 15, 16] based on the improvement of the finite element discretization or the use of specific assumptions.

Another way to reduce the complexity of the models is to develop a Component Mode Synthesis (CMS) technique [17, 18, 19, 20] for structures involving porous materials. The CMS technique consists in dividing an aggregate structure into substructures on which a modal analysis technique is individually performed. The first modes of each substructure are only considered and attachment

modes associated to the static response of the non preserved modes are added to obtain a global modal basis of the whole structure. Many reviews on the subject have been undertaken [17, 18, 19, 20, 21, 22, 23] and the reader can refer to them.

CMS techniques where mainly used for solid and fluid structures but their application to porous material is more recent [24, 25, 26] and only devoted to the case of single porous structure. Sgard *et al.* [26] proposed a decoupled modal analysis for mixed formulations which appears limited for three dimensional problems and never applied to coupled systems. Dazel *et al.* [24, 25] proposed a generalized complex modes technique for poroelastic problems for $\{\mathbf{u}^s, P\}$ problems. More recently the authors present a new displacement formulation [27] (called total formulation or $\{\mathbf{u}^s, \mathbf{u}^t\}$ formulation) and resolution techniques based on normal modes. The difference between these last two approaches first lies in the simplicity to compute the eigenmodes of the problem: the first technique was based on an extended space and complex modes as the second one is based on normal modes, easier to compute for a non-specialist.

The purpose of this paper is to propose a free interface CMS technique based on normal modes to calculate the forced response of structures involving porous materials. This technique is based on classical concept of substructuring techniques but the originality is to apply it to the case of frequency dependent problems. Normal modes associated based on the discretized spatial operators of each phase are first computed so as to avoid frequency dependent coefficients. As a selection of them is not sufficient to approximate the solution of the problem, attachment modes are added. Some of them are associated to junction degrees of freedom and others are associated to the excitation (also considered in references [21, 22]). Modal shapes are multiplied and combined at each frequency to take into account for frequency dependent coefficients. A second originality of this paper is to propose an automatic selection procedure. It is then successfully applied to monodimensional problems.

Section 2 presents the CMS technique of interest. The technique is then applied to a porous-porous (resp. porous-air) multilayered problem in section 3 (resp. 4). Section 5 concludes the paper.

## 2. Theoretical part

### 2.1. Discrete nodal problem

The structure of interest is composed of only 2 substructures. In all the paper and so as to simplify reading of the manuscript, notations relative to the second substructure correspond to the primed of the ones of the first substructure; they thereby won't be defined explicitly. If more than 2 substructures are involved, generalization of this methodology can be proceeded. The discrete problem in the frequency domain can be written in the form

$$\left[\begin{array}{ccc|c} [\mathbf{A}] & [\mathbf{0}] & [\lambda] \\ [\mathbf{0}] & [\mathbf{A}'] & [\lambda'] \\ \hline [\lambda]^t & [\lambda']^t & [\mathbf{0}] \end{array}\right] \left\{\begin{array}{c} \mathbf{u} \\ \mathbf{u}' \\ \mathbf{f} \end{array}\right\} = \left\{\begin{array}{c} \mathbf{F} \\ \mathbf{F}' \\ \mathbf{0} \end{array}\right\}. \quad (1)$$

$\mathbf{u}$ is the discretized field vector (or physical coordinates vector) of length $n$, $[\mathbf{A}]$ is the discrete matrix of the first substructure and $\mathbf{F}$ is the external force acting on the first substructure. In equation (1), Lagrange multipliers are involved to ensure continuity relations (force and displacement) at the interface between the two substructures. The number of these relations correspond to the number of degrees of freedom at the interface and is denoted by $n_j$. This number is rather small compared to $n$ and $n'$. $\mathbf{f}$ is an additional unknown vector of length $n_j$ associated to the coupling conditions and $-[\lambda][\mathbf{f}]$ can be interpreted as the force from substructure 2 on substructure 1.

### 2.2. Modal representation

This paragraph presents the formal modal decomposition of substructure 1. The discrete modal decomposition in the frequency domain of the response $\mathbf{u}(\mathbf{E}, \omega)$ to an excitation $\mathbf{E}$ can be written in the following form:

$$\mathbf{u}(\mathbf{E}, \omega) = \underbrace{\sum_{i=1}^{m} \mathbf{\Phi}_i q_i(\mathbf{E}, \omega)}_{\mathbf{S}(\mathbf{E},\omega)} + \underbrace{\sum_{i=m+1}^{n} \mathbf{\Phi}_i q_i(\mathbf{E}, \omega)}_{\mathbf{H}(\mathbf{E},\omega)}. \quad (2)$$

$\mathbf{\Phi}_i$ $(i = 1..n)$ are the eigenmodes and $q_i$ $(i = 1..n)$ are the modal coordinates. From a purely mathematical point of view, there is equivalence between the problem in physical or modal coordinates as far as the modal basis $[\mathbf{\Phi}] = [\mathbf{\Phi}_i]_{i\,(i=1..n)}$ is complete. In most cases, these modes are the first one (i.e. the one with the lowest eigen-frequencies). The other modes only contribute through their flexibility.

Excitation force $\mathbf{E}$ on substructure 1 is the sum of the two following terms: $\mathbf{F}$ is associated to known external excitation and $\hat{\mathbf{F}}$ to interaction forces with substructure 2. This second force has $n_j$ non-null components. Let $\boldsymbol{\xi}$ be the vector of length $n_j$ of the unknown forces at the interface. One has

$$\hat{\mathbf{F}} = \left[\mathbf{1}_j\right]\boldsymbol{\xi}, \quad (3)$$

with $[\mathbf{1}_j]$ the $n \times n_j$ matrix in which $\mathbf{1}_j$ corresponds to a boolean vector of length $n$ in which the only non null value is associated to $dof\ j$ of the interface. One then obtains $n_j + 1$ additional modes (called attachment modes); $n_j$ of them (denoted by $\mathbf{H}(\mathbf{1}_j, 0)$) are associated with the interface and one (denoted by $\mathbf{H}(\mathbf{F}, 0)$) associated to the external excitation.

The discrete displacement field can then be approximated by

$$\mathbf{u}(\mathbf{E}, \omega) \approx \sum_{i=1}^{m} \mathbf{\Phi}_i q_i + \mathbf{H}(\mathbf{F}, 0) q_F + \left[\mathbf{H}(\mathbf{1}_j, 0)\right]\boldsymbol{\xi}. \quad (4)$$

$q_F$ is the unknown contribution of the attachment mode associated to the excitation. Note that this contribution is

equal to 1 at zero frequency. $[\underline{\mathbf{\Phi}}]$ corresponds to the matrix of the first $m$ modes of substructure 1. Attachment mode associated to the force $\mathbf{H}(\mathbf{F},0)$ is added to the modal family. $\underline{\mathbf{q}}$ is the $m+1$ unknown vector of contributions of the modes.

### 2.3. General modal resolution procedure

Problem (1) can be rewritten in the following form:

$$\left[\begin{array}{c|c} [\mathbf{A}] & [\mathbf{0}] \\ [\mathbf{0}] & [\mathbf{A}'] \\ \hline [\lambda]^t & [\lambda']^t \end{array}\right] \left\{\begin{array}{c} \mathbf{u} \\ \mathbf{u}' \end{array}\right\} = \left\{\begin{array}{c} \mathbf{F}+\hat{\mathbf{F}} \\ \mathbf{F}'+\hat{\mathbf{F}}' \\ \mathbf{0} \end{array}\right\},$$
$$\hat{\mathbf{F}} = -[\lambda][\mathbf{f}], \quad \hat{\mathbf{F}}' = -[\lambda'][\mathbf{f}]. \tag{5}$$

$\hat{\mathbf{F}}$ and $\hat{\mathbf{F}}'$ are the interaction forces between the substructures and have non null values only at the degree of freedom corresponding to the interface (and although they are in the right hand side of equation (5), they remain unknowns of the problem).

As interaction forces are unknowns of the problem, elimination should be done. Continuities of displacements corresponds to the last row-block of problem (5) and one has

$$\begin{aligned} &\left[\underline{\mathbf{\Phi}}_b|\mathbf{H}_b(\mathbf{F},0)\right]\underline{\mathbf{q}} + \left[\mathbf{H}_b(\mathbf{1}_j,0)\right]\boldsymbol{\xi} \\ &+ \left[\underline{\mathbf{\Phi}}'_b|\mathbf{H}'_b(\mathbf{F}',0)\right]\underline{\mathbf{q}}' + \left[\mathbf{H}'_b(\mathbf{1}'_j,0)\right]\boldsymbol{\xi}' = \mathbf{0}, \end{aligned} \tag{6}$$

with

$$\begin{aligned} &\left[\mathbf{H}_b(\mathbf{1}_j,0)\right] = [\lambda]^t\left[\mathbf{H}(\mathbf{1}_j,0)\right] \\ &\left[\underline{\mathbf{\Phi}}_b\right] = [\lambda]^t\left[\underline{\mathbf{\Phi}}\right], \quad \mathbf{H}_b(\mathbf{F},0) = [\lambda]^t\mathbf{H}(\mathbf{F},0). \end{aligned} \tag{7}$$

Interaction force vector $\boldsymbol{\xi}$ is then solution of the problem

$$\begin{aligned} &\underbrace{\left(\left[\mathbf{H}'_b(\mathbf{1}'_j,0)\right] - \left[\mathbf{H}_b(\mathbf{1}_j,0)\right]\right)}_{[\mathbf{R}_b]}\boldsymbol{\xi} \\ &= \left[\underline{\mathbf{\Phi}}_b|\mathbf{H}_b(\mathbf{F},0)\right]\underline{\mathbf{q}} + \left[\underline{\mathbf{\Phi}}'_b|\mathbf{H}'_b(\mathbf{F}',0)\right]\underline{\mathbf{q}}'. \end{aligned} \tag{8}$$

$[\mathbf{R}_b]$ is a $n_j \times n_j$ matrix which can be inverted to express $\boldsymbol{\xi}$ as a function of the modal contributions. The nodal displacements are finally given by

$$\left\{\begin{array}{c} \mathbf{u} \\ \mathbf{u}' \end{array}\right\} \approx \left[\mathbf{\Psi}\right] \left\{\begin{array}{c} \underline{\mathbf{q}} \\ \underline{\mathbf{q}}' \end{array}\right\}, \tag{9}$$

with

$$\begin{aligned} \left[\mathbf{\Psi}\right] = &\left[\begin{array}{c|c} [\underline{\mathbf{\Phi}}|\mathbf{H}(\mathbf{F},0)] & [\mathbf{0}] \\ \hline [\mathbf{0}] & [\underline{\mathbf{\Phi}}'|\mathbf{H}'(\mathbf{F}',0)] \end{array}\right] \\ &+ \left[\begin{array}{c|c} \left[\mathbf{H}(\mathbf{1}_j,0)\right]\left[\mathbf{R}_b\right]^{-1}\left[\underline{\mathbf{\Phi}}_b|\mathbf{H}_b(\mathbf{F},0)\right] & \\ \hline -\left[\mathbf{H}'(\mathbf{1}'_j,0)\right]\left[\mathbf{R}_b\right]^{-1}\left[\underline{\mathbf{\Phi}}_b|\mathbf{H}_b(\mathbf{F},0)\right] & \end{array}\right. \\ &\left.\begin{array}{c|} \\ \hline \left[\mathbf{H}(\mathbf{1}_j,0)\right]\left[\mathbf{R}_b\right]^{-1}\left[\underline{\mathbf{\Phi}}'_b|\mathbf{H}'_b(\mathbf{F}',0)\right] \\ \hline -\left[\mathbf{H}'(\mathbf{1}'_j,0)\right]\left[\mathbf{R}_b\right]^{-1}\left[\underline{\mathbf{\Phi}}'_b|\mathbf{H}'_b(\mathbf{F}',0)\right] \end{array}\right]. \end{aligned} \tag{10}$$

For any contributions $\underline{\mathbf{q}}$ and $\underline{\mathbf{q}}'$, the methodology ensures the continuity relations on displacement and force for the unknown nodal vector in (9). The projection of problem (1) in which Lagrange multipliers, now useless, are omitted on the $[\mathbf{\Psi}]$ family leads to a reduced problem.

This technique is called FICMT (Force Interface Corrected Modal Technique). In order to evaluate its accuracy, it is compared to methods of the literature. If attachment modes $\mathbf{H}(\mathbf{F},0)$ are not considered, only the correction at the interface is taken into account; it corresponds to Craig and Chang technique [17, 18] and this technique is denoted ICMT (Interface Corrected Modal Technique). If no correction is considered (Direct Modal Technique or DMT), problem (1) is projected on the matrix of free-modes aggregated with an identity matrix for Lagrange multipliers.

### 2.4. Automatic selection of the modes

One key point of modal techniques is to find the adequate number of modes in the selection of each modal basis. Some empirical criterion are often used (as for example to preserve modes with eigenfrequencies lower to twice the frequency of excitation). In this section an automatic selection procedure is proposed. The idea of the method is to compare the accuracy of the modal solution in terms of residual.

Let $\check{\mathbf{U}}$ (displacement vector (of length $n-n_j$) of the first substructure of degrees of freedom which do not belong to the boundary), $\check{\mathbf{U}}_b$ (common displacement vector) be the solution of the modal problem obtained with a selection of $m$ and $m'$ modes. One residual vector can be computed for each substructure,

$$\begin{aligned} \mathbf{R} &= \left[\begin{array}{c|c} [\check{\mathbf{A}}] & [\mathbf{0}] \\ \hline [\mathbf{0}] & [\check{\mathbf{A}}_b] \end{array}\right] \left\{\begin{array}{c} \check{\mathbf{U}} \\ \check{\mathbf{U}}_b \end{array}\right\} - \left\{\begin{array}{c} \check{\mathbf{F}} \\ \check{\mathbf{F}}_b \end{array}\right\} \\ \mathbf{R}' &= \left[\begin{array}{c|c} [\check{\mathbf{A}}_b] & [\mathbf{0}] \\ \hline [\mathbf{0}] & [\check{\mathbf{A}}'] \end{array}\right] \left\{\begin{array}{c} \check{\mathbf{U}}_b \\ \check{\mathbf{U}}' \end{array}\right\} - \left\{\begin{array}{c} \check{\mathbf{F}}_b \\ \check{\mathbf{F}}' \end{array}\right\}. \end{aligned} \tag{11}$$

These residuals (which should be null if the displacements correspond to the exact ones) allow to control the number of modes for each substructure. There is a need of two scalar parameters $\varepsilon$ and $\varepsilon'$ that must be chosen. If $\|\mathbf{R}\| > \varepsilon$, the number of modes for the first substructure is not sufficient and $m$ is incremented. Similar procedure can be done for second substructure. Hence, the modal families can be selected separately for the two substructures. In the case of a bandwidth frequency resolution, the method is as follows. 1 mode is selected for both substructures and the modal resolution is undertaken. If the criterion condition are verified the following frequency is considered. In the other case a mode is added to the substructure having the maximum $\|\mathbf{R}\|/\varepsilon$ ratio and the modal resolution is done another time. The procedure is continued until the criterion are reached for both substructures; when it is the case the following frequency is considered. Choice of $\varepsilon$ and $\varepsilon'$ is crucial and is the key point of this automatic selection procedure. Examples are given in the application section.

## 3. Porous-porous structure

In this section, the monodimensional problem (depicted in Figure 1) of two porous structures bonded onto a hard

backing is studied. Each piece, of thickness 2 cm, is discretized by finite-element using the $\{\mathbf{u}^s, \mathbf{u}^t\}$ formulation. $N$ and $N'$ elements are respectively considered for the first and second layer. Properties of the media are given in Table I.

### 3.1. Discretized problem in physical coordinates

The nodal problem (1) for the case of interest reads [13]

$$\left( \left[\begin{array}{cc|cc|cc} \hat{P}[\mathbf{K}_0] & [\mathbf{0}] & [\mathbf{0}] & [\mathbf{0}] & \lambda_s & \mathbf{0} \\ [\mathbf{0}] & \widetilde{K}_{eq}[\mathbf{K}_0] & [\mathbf{0}] & [\mathbf{0}] & \mathbf{0} & \lambda_t \\ \hline [\mathbf{0}] & [\mathbf{0}] & \hat{P}'[\mathbf{K}'_0] & [\mathbf{0}] & \lambda'_s & \mathbf{0} \\ [\mathbf{0}] & [\mathbf{0}] & [\mathbf{0}] & \widetilde{K}'_{eq}[\mathbf{K}'_0] & \mathbf{0} & \lambda'_t \\ \hline \lambda_s^t & \mathbf{0}^t & \lambda_s'^t & \mathbf{0}^t & 0 & 0 \\ \mathbf{0}^t & \lambda_t^t & \mathbf{0}^t & \lambda_t'^t & 0 & 0 \end{array}\right] - \omega^2 \left[\begin{array}{cc|cc|cc} \widetilde{\rho}_s[\mathbf{M}_0] & \widetilde{\gamma}\widetilde{\rho}_{eq}[\mathbf{M}_0] & [\mathbf{0}] & [\mathbf{0}] & \mathbf{0} & \mathbf{0} \\ \widetilde{\gamma}\widetilde{\rho}_{eq}[\mathbf{M}_0] & \widetilde{\rho}_{eq}[\mathbf{M}_0] & [\mathbf{0}] & [\mathbf{0}] & \mathbf{0} & \mathbf{0} \\ \hline [\mathbf{0}] & [\mathbf{0}] & \widetilde{\rho}'_s[\mathbf{M}'_0] & \widetilde{\gamma}'\widetilde{\rho}'_{eq}[\mathbf{M}'_0] & \mathbf{0} & \mathbf{0} \\ [\mathbf{0}] & [\mathbf{0}] & \widetilde{\gamma}'\widetilde{\rho}'_{eq}[\mathbf{M}'_0] & \widetilde{\rho}'_{eq}[\mathbf{M}'_0] & \mathbf{0} & \mathbf{0} \\ \hline \mathbf{0}^t & \mathbf{0}^t & \mathbf{0}^t & \mathbf{0}^t & 0 & 0 \\ \mathbf{0}^t & \mathbf{0}^t & \mathbf{0}^t & \mathbf{0}^t & 0 & 0 \end{array}\right] \right) \cdot \left\{\begin{array}{c} \mathbf{u}_s \\ \mathbf{u}_t \\ \mathbf{u}'_s \\ \mathbf{u}'_t \\ f_s \\ f_t \end{array}\right\} = \left\{\begin{array}{c} \mathbf{F}_s \\ \mathbf{F}_t \\ \mathbf{F}'_s \\ \mathbf{F}'_t \\ 0 \\ 0 \end{array}\right\} \tag{12}$$

Physical parameters are obtained with the Biot-Allard theory and expressions can be found in Appendix A1. For each porous structure solid and total displacement are discretized with linear finite element and the same mesh is used. The values of $[\mathbf{K}_0]$ and $[\mathbf{M}_0]$ can be found in Appendix A2. Dirichlet conditions are imposed on the second substructure; hence $n = 2(N+1)$ and $n' = 2N'$. $\mathbf{u}_s$ and $\mathbf{u}_t$ (resp. $\mathbf{u}'_s$ and $\mathbf{u}'_t$) correspond to the solid and total displacement nodal vector which are both of length $N+1$ (resp. $N'$) for the first (resp. second) substructure. As $\{\mathbf{u}^s, \mathbf{u}^t\}$ formulation [13] is considered the continuity relations are simple and $\lambda_s = \lambda_t$ (resp. $\lambda'_s = \lambda'_t$) is a vector of length $N+1$ (resp. $N'$) whose only non-null component is 1 (resp. $-1$) at the last (resp. the first) index. Hence, the last two lines correspond to the continuity of the solid and total displacements. $f_s$ and $f_t$ correspond to interaction forces (for the solid in-vacuo and the pressure) and are both scalar unknowns of the problem. Concerning forces in the right hand side, the only non-null value is a unit force on the first degree of freedom of $\mathbf{F}_t$.

### 3.2. Modal shapes of the problem and DMT

The eigenmodes $[\mathbf{\Phi}]$ of the first substructure are obtained by solving the generalized eigenvalue problem associated to matrix $[\mathbf{K}_0]$ and $[\mathbf{M}_0]$. The eigenvectors are normalized with respect to $[\mathbf{M}_0]$ so that $[\mathbf{\Phi}]^t[\mathbf{M}_0][\mathbf{\Phi}]$ is the identity matrix and $[\mathbf{\Phi}]^t[\mathbf{K}_0][\mathbf{\Phi}]$ is the diagonal matrix $[\mathbf{k}^2]$ of the eigenvalues $k_i^2$. Note that for this first substructure a rigid body mode exists whose displacements are all equal. For

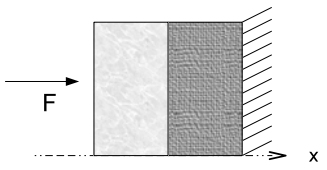


Figure 1. Configuration of the problem.

each one of the porous, the solid and total displacements should be approximated by a modal decomposition. If no correction is applied for non preserved modes (DMT), displacements are expressed in their modal form and Lagrange multipliers are kept. Hence, one has

$$\left\{\begin{array}{c} \underline{\mathbf{u}}_s \\ \underline{\mathbf{u}}_t \\ \underline{\mathbf{u}}'_s \\ \underline{\mathbf{u}}'_t \\ f_s \\ f_t \end{array}\right\} = \left[\begin{array}{ccccc} [\underline{\mathbf{\Phi}}] & [\mathbf{0}] & [\mathbf{0}] & [\mathbf{0}] & [\mathbf{0}] \\ [\mathbf{0}] & [\underline{\mathbf{\Phi}}] & [\mathbf{0}] & [\mathbf{0}] & [\mathbf{0}] \\ [\mathbf{0}] & [\mathbf{0}] & [\underline{\mathbf{\Phi}}'] & [\mathbf{0}] & [\mathbf{0}] \\ [\mathbf{0}] & [\mathbf{0}] & [\mathbf{0}] & [\underline{\mathbf{\Phi}}'] & [\mathbf{0}] \\ [\mathbf{0}] & [\mathbf{0}] & [\mathbf{0}] & [\mathbf{0}] & [\mathbf{I}_2] \end{array}\right] \left\{\begin{array}{c} \underline{\mathbf{q}}_s \\ \underline{\mathbf{q}}_t \\ \underline{\mathbf{q}}'_s \\ \underline{\mathbf{q}}'_t \\ f_s \\ f_t \end{array}\right\}. \tag{13}$$

In all the paper $[\mathbf{I}_k]$ denotes the identity matrix of size $k$. The same number of modes is preserved for the solid and total displacement and the modal matrix of (13) is of size $(2(N+N'+1) \times 2(M+M'+1))$.

### 3.3. Attachment modes, frequency dependance, ICMT and FICMT

The first step of ICMT and FICMT is to calculate the attachment modes associated to the static contributions of non preserved modes. For the problem of interest, 5 attachment modes need to be calculated. Concerning substructure 1, one attachment mode related to excitation is needed. For both substructures, two attachment modes are associated to the interface, the first (resp. second) one corresponding to the *in-vacuo* excitation (resp. the pressure). It can be shown that this first and second attachment modes are proportional with respect to elastic coefficients. Hence, the method to obtain them is first to compute solutions associated to shape matrices $[\mathbf{K}_0]$ and $[\mathbf{K}'_0]$ and then to divide by the adequate elastic modulus.

Concerning substructure 1, $[\mathbf{K}_0]$ is not invertible as the first mode $\mathbf{\Phi}_1$ is not elastic but a constant displacement rigid body motion. To avoid this problem, let now consider the following matrices:

$$\begin{aligned} \left[\mathbf{P}\right] &= \left[\mathbf{I}_{n+1}\right] - \mathbf{\Phi}_1\mathbf{\Phi}_1^t\left[\mathbf{M}_0\right] \\ \left[\mathbf{K}_0^P\right] &= \left[\mathbf{P}\right]^t\left[\mathbf{K}_0\right]\left[\mathbf{P}\right], \quad \mathbf{F}_t^P = \left[\mathbf{P}\right]^t\mathbf{F}_t. \end{aligned} \tag{14}$$

$[\mathbf{P}]$ is a projection matrix which filter the rigid mode $\mathbf{\Phi}_1$. $[\mathbf{K}_0^P]$ is not invertible but let $\mathbf{u}^P$ be the displacement vector of length $N$ obtained while solving the problem obtained by removing last line and column of $[\mathbf{K}_0^P]$ as well as the

last line of $\mathbf{F}_i^P$. One then defines

$$\mathbf{u}_F = \left[\mathbf{P}\right] \left\{ \begin{array}{c} \mathbf{u}^P \\ 0 \end{array} \right\}, \quad \mathbf{S}_F = \sum_{i=2}^{m} \frac{\mathbf{F}_t^t}{{k_i}^2} \mathbf{\Phi}_i$$
$$\mathbf{H}_F = \mathbf{u}_F - \mathbf{S}_F. \tag{15}$$

$\mathbf{H}_F$ is not exactly the static contribution of higher modes at frequency $\omega$ but it has to divided by a compressibility. As $\widetilde{K}_{eq}$ is frequency dependent, this should be done with care. The modal contributions $q_i^s$ and $q_i^t$ at frequency $\omega$ to modal forces $F_i^s$ and $F_i^t$ are solution of the equations [13]

$$\begin{aligned} \hat{P} k_i^2 q_i^s - \omega^2 (\widetilde{\rho}_s q_i^s + \widetilde{\gamma}\widetilde{\rho}_{eq} q_i^t) &= F_i^s, \quad , \\ \widetilde{K}_{eq} k_i^2 q_i^t - \omega^2 (\widetilde{\gamma}\widetilde{\rho}_{eq} q_i^s + \widetilde{\rho}_{eq} q_i^t) &= F_i^t. \end{aligned} \tag{16}$$

Neglecting inertial effects induces that $q_i^s = F_i^s / \hat{P} k_i^2$ and $q_i^t = F_i^t / \widetilde{K}_{eq} k_i^2$. These two relations indicates that the elastic properties that should be considered are the one of the current frequency and not the one at null frequency. Hence, $\mathbf{H}_F$ should be divided by $\widetilde{K}_{eq}$ to obtain the attachment mode.

While applying symmetry and linearity properties, it is straightforward to calculate the pressure (resp. *in-vacuo*) attachment mode $\mathbf{H}_0 / \widetilde{K}_{eq}$ (resp. $\mathbf{H}_0 / \hat{P}$) at the interface between porous 1 and 2.

For second substructure, let now define

$$\mathbf{u}_0' = [\mathbf{K}_0']^{-1} \mathbf{1}_1', \quad \mathbf{S}_0' = \sum_{i=1}^{n'} \frac{\mathbf{\Phi}_i'(1)}{{k_i'}^2} \mathbf{\Phi}_i'$$
$$\mathbf{H}_0' = \mathbf{u}_0' - \mathbf{S}_0'. \tag{17}$$

$[\mathbf{K}_0']$ is real symmetric and positive-definite so that there is no problem of existence in the preceding equations.

Hence, it is now possible to build the matrices and vectors of eq. (9). In the following equations, index in parenthesis corresponds to the dimension of vectors and matrices.

$$\mathbf{H}(\mathbf{F}, 0) = \left\{ \begin{array}{c} \mathbf{0}_{N+1} \\ \hline \dfrac{\mathbf{H}_F}{\widetilde{K}_{eq}} \end{array} \right\}_{(2N+2\times 1)}$$
$$\mathbf{H}_b(\mathbf{F}, 0) = \left\{ \begin{array}{c} 0 \\ \hline \dfrac{\mathbf{H}_F(N+1)}{\widetilde{K}_{eq}} \end{array} \right\}_{(2\times 1)}. \tag{18}$$

The $N+1$ index is associated to the last $dof$ of substructure 1 which corresponds to the interface. For both substructures two attachment modes are needed; the first (resp. second) one is associated to the continuity of the in-vacuo (resp. pressure) force,

$$\left[\mathbf{H}(\mathbf{1}_j, 0)\right] = \left[ \begin{array}{cc} \dfrac{\mathbf{H}_0}{\hat{P}} & \mathbf{0} \\ \mathbf{0} & \dfrac{\mathbf{H}_0}{\widetilde{K}_{eq}} \end{array} \right]_{(2N+2\times 2)}$$
$$\left[\mathbf{H}'(\mathbf{1}_j', 0)\right] = \left[ \begin{array}{cc} \dfrac{\mathbf{H}_0'}{\hat{P}'} & \mathbf{0} \\ \mathbf{0} & \dfrac{\mathbf{H}_0'}{\widetilde{K}_{eq}'} \end{array} \right]_{(2N'\times 2)}. \tag{19}$$

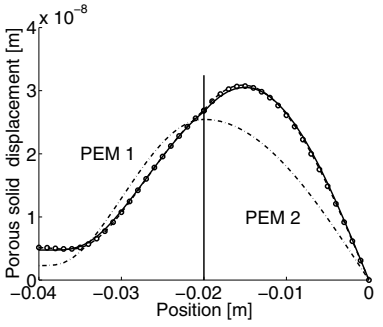


Figure 2. Solid displacement of the two porous structures. Solid: analytical solution; Dash-dot: DMT; Dash: ICMT; Circles: FICMT.

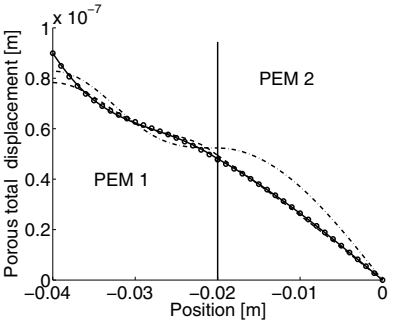


Figure 3. Total displacement of the two porous structures. Solid: analytical solution; Dash-dot: DMT; Dash: ICMT; Circles: FICMT.

As two continuity conditions are involved, $[\mathbf{R}_b]$ is a $2 \times 2$ matrix,

$$\left[\mathbf{R}_b\right] = \left[ \begin{array}{cc} \dfrac{\mathbf{H}_0(N+1)}{\hat{P}} + \dfrac{\mathbf{H}_0'(1)}{\hat{P}'} & \mathbf{0} \\ \mathbf{0} & \dfrac{\mathbf{H}_0(N+1)}{\widetilde{K}_{eq}} + \dfrac{\mathbf{H}_0'(1)}{\widetilde{K}_{eq}'} \end{array} \right]_{(2\times 2)}. \tag{20}$$

This matrix is diagonal due to the decoupling of in-vacuo stress and pressure in $\{\mathbf{u}^s, \mathbf{u}^t\}$ formulation. The first index of the second substructure is associated to the interface and the modal matrices at the boundary read:

$$\left[\underline{\mathbf{\Phi}}_b\right] = \left[ \begin{array}{c|c} \underline{\mathbf{\Phi}}(N+1) & \mathbf{0} \\ \hline \mathbf{0} & \underline{\mathbf{\Phi}}(N+1) \end{array} \right]_{(2\times 2m)}$$
$$\left[\underline{\mathbf{\Phi}}_b'\right] = \left[ \begin{array}{c|c} -\underline{\mathbf{\Phi}}'(1) & \mathbf{0} \\ \hline \mathbf{0} & -\underline{\mathbf{\Phi}}'(1) \end{array} \right]_{(2\times 2m')}. \tag{21}$$

Now, all elements of problem (9) are known. Modal solutions though ICMT and FICMT can be obtained.

### 3.4. Results

Figure 2 and 3 respectively present the solid and total displacement of the structures at 1500 Hz. 2 modes are used

Table I. Parameters of porous material *A* and *B*.

| Mat | Porosity $\phi$ | Flow resistivity $\sigma$ (N m$^{-4}$ $s$) | Tortuosity $\alpha_\infty$ | Viscous characteristic length $\Lambda$ (m) | Thermal characteristic length $\Lambda'$ (m) |
|---|---|---|---|---|---|
| A | 0.97 | 87000 | 1.52 | $3.7\ 10^{-5}$ | $1.2\ 10^{-4}$ |
| B | 0.97 | 40000 | 1.06 | $0.56\ 10^{-4}$ | $0.112\ 10^{-3}$ |
| Mat | | Density $\rho_1$ (kg m$^{-3}$) | Young's modulus $E$ (Pa) | Loss factor $\eta_s$ | Poisson coefficient $\nu$ |
| A | | 31 | $1.43\ 10^7$ | 0.055 | 0.3 |
| B | | 130 | $0.44\ 10^7$ | 0.3 | 0.1 |

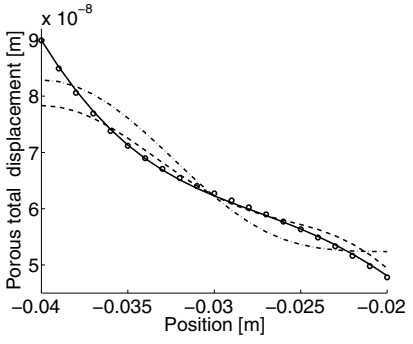


Figure 4. Total displacement of the two porous structures, detail near the excitation. Solid: analytical solution; Dash-dot: DMT; Dash: ICMT; Circles: FICMT.

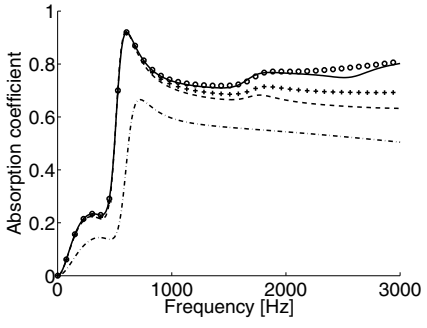


Figure 5. Absorption coefficient versus frequency for 1 mode in each porous substructure. Solid: analytical solution; Dash-dot: DMT; Dash: ICMT; Circles: FICMT; Plus: FICMT under assumption that the contribution of the attachment mode associated to the force is 1.

for the the first substructure and 1 mode is considered for the second substructure. For the solid displacement the ICMT and the proposed approach perfectly match with the analytical solution. For these two methods, the correction at the interface between the two porous materials allows a non null stress at the interface. For the DMT, one can observe that the space derivative of the displacement at the interface is null. It is a consequence of the only use of free interface modes. A similar remark can be done for the force correction: The space derivative of the total displacement is null at the left interface for DMT an ICMT while it coincides for the FICMT. Concerning the displacement shape, the difference between the ICMT and the FICMT is more important for the total displacement than for the solid one (At the air-porous interface, the difference is equal to 15% for the total displacement and a detail on the left substructure for the total displacement is provided in Figure 4). This can be understood as the force correction concerns the pressure for the case of interest.

Figure 5 represents the absorption coefficient as a function of frequency. The first resonance is at 600 Hz and the second one at 1800 Hz. The three modal techniques are compared and for each one of them only 1 mode in each substructure is considered. It can be noticed that the DMT does not provide accurate results in this case. The ICMT agrees till the first resonance, and then diverges from the analytical solution and the FICMT is in good agreement till the second resonance. Hence the static correction for the contribution of higher modes to the excitation allows to maintain the performance of the technique in a additional 700 Hz frequency range. After the second resonance there is a need for an additional mode and there is no doubt that the resonance of a mode cannot be replaced by a static correction. As intermediate conclusion, it appears that the FICMT is the most accurate techniques among these three and that it is able to limit the number of kept modes to the adequate ones.

The automatic selection procedure is now studied and this method is only studied for the case of FICMT technique as the two other techniques are less accurate. Figure 6 (resp. 7 represents the evolution of the residual error $\varepsilon_1$ and $\varepsilon_2$ (resp. the number of preserved modes for the first and second substructure) as a function of frequency. For frequencies lower to 555 Hz, only one mode were retained for both structures. In this range the residual error increases with frequency until the residual error on the left substructure reach the tolerance. A mode is the added to the left part. This induces a huge decrease of the residual error of the first substructure. Even if the range of the figure does make it noticeable, the error on the second substructure also decreases (from 0.0198 to 0.0168). In the second frequency part, 2 modes are considered for the left structure and one for the right one. It can also be noticed that the error is not always increasing with the frequency.

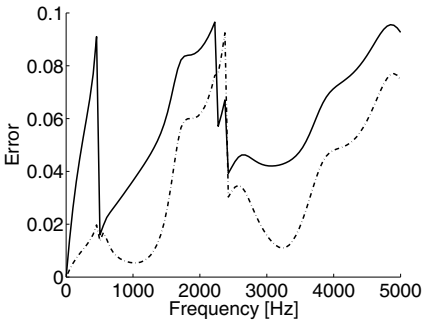


Figure 6. Error with a truncation criterion on the residual $\varepsilon_1 = \varepsilon_2 = 0.1$. Solid: Error relative to the left substructure; Dash-dot: Error relative to the right substructure.

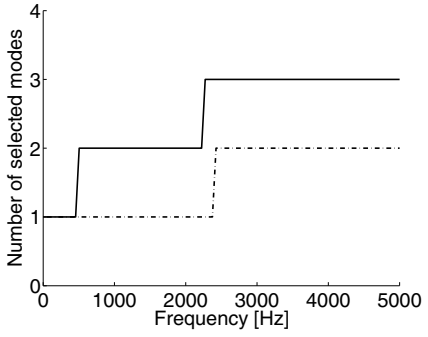


Figure 7. Number of selected modes versus frequency. Solid: Modes of the left substructure $\varepsilon = 0.1$; Dash-dot: Modes of the right substructure $\varepsilon = 0.1$.

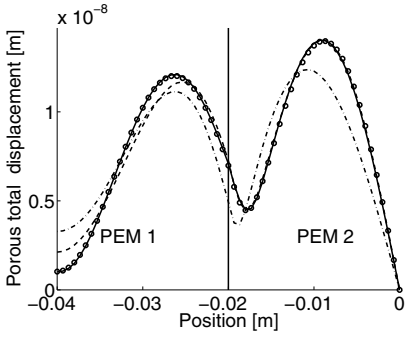


Figure 8. Total displacement at 2300 Hz. Solid: Analytical solution; Dash-dot: Solution with (2;1) modes; Dash: Solution with (2;2) modes; Circles: Solution with (3;2) modes.

Around 2300 Hz several modes are added; one to the left at 2270 Hz and one to the right at 2420 Hz. The total displacement shape is plotted at 2300 Hz in figure 8 for different number of modes to understand the influence of added modes.

Figure 9 proposes the error on the absorption coefficient as a function of frequency for different values of the residual error criterion. It can be noticed that this error does

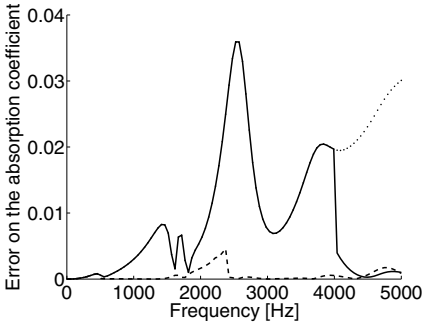


Figure 9. Error on the absorption coefficient versus frequency. Dash: $\varepsilon = 0.1$; Solid: $\varepsilon = 0.5$; Dot: $\varepsilon = 2$.

not coincide with the residual one (there is no mathematical or physical reason for this). Nevertheless, the more the residual criterion is weak and the lower is the error on the absorption coefficient. Nevetheless, for this problem, errors are very weak (it was shown that 1 mode in each substructure is sufficient until 1800 Hz.).

## 4. Case of porous-air structure

The monodimensional problem of one porous layer lying over an air plenum is studied. This problem is the same than the one of the preceding section and depicted in Figure 1 but the second porous layer is replaced by an air cavity. The porous layer is discretized by finite-element using the $\{\mathbf{u}^s, \mathbf{u}^t\}$ formulation. The air medium is discretized using displacement formulation and $\mathbf{u}_a$ denotes the $dof$ vector. As there is analogy between this problem and the preceding one, similar notations are used.

### 4.1. Implementation of the problem

Nodal problem in physical coordinates reads

$$\left( \left[\begin{array}{ccc|c} \hat{P}[\mathbf{K}_0] & [\mathbf{0}] & [\mathbf{0}] & \mathbf{0}_s \\ [\mathbf{0}] & \widetilde{K}_{eq}[\mathbf{K}_0] & [\mathbf{0}] & \lambda_t \\ \hline [\mathbf{0}] & [\mathbf{0}] & K_0[\mathbf{K}'_0] & \lambda'_a \\ \hline \mathbf{0}_s^t & \lambda_t^t & \lambda_a'^{\,t} & 0 \end{array}\right] \cdots \right.$$

$$\left. - \omega^2 \left[\begin{array}{cc|c|c} \widetilde{\rho}_s[\mathbf{M}_0] & \widetilde{\gamma}\widetilde{\rho}_{eq}[\mathbf{M}_0] & [\mathbf{0}] & \mathbf{0}_s \\ \widetilde{\gamma}\widetilde{\rho}_{eq}[\mathbf{M}_0] & \widetilde{\rho}_{eq}[\mathbf{M}_0] & [\mathbf{0}] & \mathbf{0}_t \\ \hline [\mathbf{0}] & [\mathbf{0}] & \rho_0[\mathbf{M}'_0] & \mathbf{0}_a \\ \hline {}^t\mathbf{0}_s & {}^t\mathbf{0}_t & {}^t\mathbf{0}_a & 0 \end{array}\right] \right) \cdot \left\{\begin{array}{c} \mathbf{u}_s \\ \mathbf{u}_t \\ \mathbf{u}_a \\ f_c \end{array}\right\} = \left\{\begin{array}{c} \mathbf{F}^s \\ \mathbf{F}^t \\ \mathbf{F}^a \\ 0 \end{array}\right\}. \quad (22)$$

$\mathbf{u}_s$ and $\mathbf{u}_t$ are both $N+1$ length and $\mathbf{u}_a$ is of size $N$. $K_0$ is the adiabatic bulk modulus of air, and $\rho_0$ is the air density. $f_c$ corresponds to interaction forces between both media. $\lambda_t$ and $\lambda'_a$ are defined similarly to the preceding section. Hence, the last line is associated to the continuity of total

and air displacements at the interface. Eigen-modes of the porous substructure are computed as proposed in section III. The eigen-modes of the air substructure are obtained by solving the generalized eigenvalue problem associated to matrix $[\mathbf{K}_a]$ and $[\mathbf{M}_a]$ . The eigenvectors are normalized with respect to $[\mathbf{M}_a]$. For DMT, displacements are expressed in their modal form and Lagrange multipliers are kept,

$$\begin{Bmatrix} \underline{\mathbf{u}}_s \\ \underline{\mathbf{u}}_t \\ \underline{\mathbf{u}}'_a \\ f_c \end{Bmatrix} = \left[\begin{array}{cc|c|c} [\underline{\mathbf{\Phi}}] & [\mathbf{0}] & [\mathbf{0}] & \mathbf{0} \\ [\mathbf{0}] & [\underline{\mathbf{\Phi}}] & [\mathbf{0}] & \mathbf{0} \\ \hline [\mathbf{0}] & [\mathbf{0}] & [\underline{\mathbf{\Phi}'}] & \mathbf{0} \\ \hline \mathbf{0}^t & \mathbf{0}^t & \mathbf{0}^t & 1 \end{array}\right] \begin{Bmatrix} \underline{\mathbf{q}}_s \\ \underline{\mathbf{q}}_t \\ \underline{\mathbf{q}}'_a \\ f_c \end{Bmatrix}. \tag{23}$$

Attachment modes linked to the excitation are independent from the second substructure; they are then not modified

$$\begin{aligned} \mathbf{H}(\mathbf{F},0) &= \begin{Bmatrix} \mathbf{0}_{N+1} \\ \mathbf{H}_F \\ \hline \widetilde{K}_{eq} \end{Bmatrix}_{(2(N+1)\times 1)} \\ \mathbf{H}_b(\mathbf{F},0) &= \begin{Bmatrix} 0 \\ \hline \dfrac{\mathbf{H}_F(N+1)}{\widetilde{K}_{eq}} \end{Bmatrix}_{(2\times 1)} . \end{aligned} \tag{24}$$

Regarding the interface, the in-vacuo force of the porous is null and only the continuity of pressure is concerned inducing that only 1 attachment mode is necessary for both structures. One has

$$\begin{aligned} \left[\mathbf{H}(\mathbf{1}_j,0)\right] &= \begin{Bmatrix} \mathbf{0}_{N+1} \\ \mathbf{H}_F \\ \hline \widetilde{K}_{eq} \end{Bmatrix}_{(2(N+1)\times 1)} \\ \left[\mathbf{H}'(\mathbf{1}'_j,0)\right] &= \begin{Bmatrix} \mathbf{H}'_0 \\ \hline K_0 \end{Bmatrix}_{(N'\times 1)} \end{aligned} \tag{25}$$

and $[\mathbf{R}_b]$ is only a scalar,

$$\left[\mathbf{R}_b\right] = \left[\frac{\mathbf{H}_0(N+1)}{\widetilde{K}_{eq}} + \frac{\mathbf{H}'_0(1)}{K_0}\right]_{(1\times 1)} . \tag{26}$$

The modal matrices at the boundary then read

$$\begin{aligned} \left[\underline{\mathbf{\Phi}}_b\right] &= \left[\underline{\mathbf{\Phi}}(N+1)\right]_{(1\times m)}, \quad , \\ \left[\underline{\mathbf{\Phi}}'_b\right] &= \left[-\underline{\mathbf{\Phi}}'(1)\right]_{(1\times m')}. \end{aligned} \tag{27}$$

### 4.2. Results

The proposed example considers a porous layer of material A and 5 cm thickness and an air plenum of 10 cm. 30 nodes are used for each substructure which ensures the convergence of the discrete model in the frequency range of the study. Properties of the material A are given in Table I. Bulk modulus $K_0$ and air density $\rho_0$ are the one corresponding to a pressure of 101300 Pa and temperature 20°C.

Figure 10 presents the total displacement at 500 Hz. Two modes are considered for porous and air. Influence of the external force correction is noticeable as the displacement at the interface: FICMT is nearly closed to the analytical solution as the error of ICMT and DMT is around 20%. Accuracy of FICMT is also shown in this example. Similarly to preceding section, Figure 11 presents the absorption coefficient as a function of frequency and Figure 12, the associated number of preserved modes with the automatic procedure. The result for $\varepsilon = 0.2$ is inter-

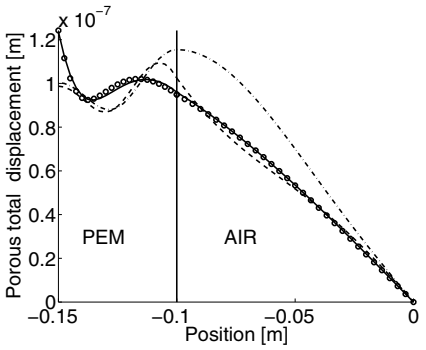


Figure 10. Total displacement of the porous structure and air displacement. Solid: analytical solution; Dash-dot: DMT; Dash: ICMT ; Circles: FICMT.

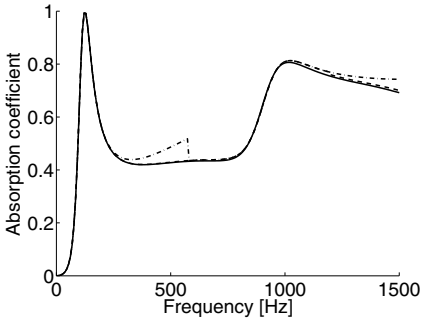


Figure 11. Absorption coefficient versus frequency. Solid: Exact solution; Dash-dot: $\varepsilon = 0.4$; Dash: $\varepsilon = 0.2$.

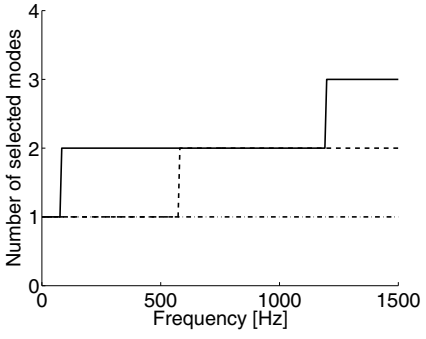


Figure 12. Number of selected modes versus frequency. Solid: Modes of the porous substructure $\varepsilon = 0.2$; Dash-dot: Modes of the air substructure $\varepsilon = 0.2$; Dash: Modes of the porous substructure $\varepsilon = 0.4$.

esting and it can be observed that modes are added near the resonances (i.e. when they contribute to the response of the structure). For $\varepsilon = 0.4$, a discontinuity is observed in the absorption coefficient. The reason is that the second mode for the porous is added after 500 Hz instead of 150 Hz. Hence, in this frequency range, the numerical cost is lower (less mode than necessary) but this has an influence on accuracy.

## 5. Conclusion

An free interface CMS technique has been proposed for the resolution of problem with coupled substructures including porous media. This technique is based on normal modes. Additional attachment modes are added in order to take into account the influence of non preserved modes. These attachment modes concern both the interface between substructures as well as the external excitation on substructures. Frequency dependence of poroelastic coefficients has been taken into account in the frequency loop. A simple criterion based on the evaluation of a residual vector has been implemented. This allows an automatic selection of the number of preserved modes.

The method has been validated in comparison with analytical model on two 1D configurations involving two layers of porous material bonded onto a hard backing or a porous layer with an air plenum to demonstrate the ability of the method to handle coupled systems. It is also compared to the direct modal technique without correction (DMT) and to the Craig and Chang technique ICMT (Interface Corrected Modal Technique) where correction is applied only at the interface. Even if results are not presented in this paper the technique has been validated on a wide range of materials. Other monodimensional configurations have been studied and confirms the convergence of the method.

It is shown that the proposed approach perfectly matches with the analytical solution for a number of modes corresponding to the one which should be excited. Considering absorption coefficient, discrepancies between different methods appear above the first resonance mode but the proposed technique matches with the analytical solution. It was necessary to consider such simple problems to ensure the validity of the method but these examples are not the best one to check for the efficiency in terms of computational cost. It is a perspective of this paper and further works consists in applying this technique to 2D and 3D problems to better quantify the efficiency of this method. In particular shear waves will be involved. It should also be applied in configurations where the substructures have a high ratio of interface to interior degree of freedom to investigate its performance.

## Appendix

## A1. Topics on Biot-Allard model

This appendix provides the expressions of the inertial and constitutive parameters of the Biot-Allard model. All these expressions can be found in Allard [1]. This model allows to find the expressions of the coefficient used in the manuscript as a function of the material properties. These expressions are given for a circular frequency $\omega$.

The density terms are first reminded. They are given by

$$\rho_1 = (1-\phi)\rho_s, \quad \rho_2 = \phi\rho_0, \quad \rho_{12} = -\phi\rho_0(\alpha_\infty - 1). \tag{A1}$$

$\phi$ is porosity, $\rho_s$ is skeleton material density, $\rho_0$ is interstitial fluid density and $\alpha_\infty$ refers to geometric tortuosity. $\rho_{12}$ accounts for the interaction between the inertia forces of the solid and fluid phase.The apparent inertial mass can be introduced:

$$\widetilde{\rho}_{12} = \rho_{12} - \frac{\widetilde{b}}{\mathrm{j}\omega}, \quad \widetilde{\rho}_{22} = \rho_2 - \widetilde{\rho}_{12}.$$

The viscous effects are modelled through $\widetilde{b}$ coefficient whose expression is

$$\widetilde{b} = \mathrm{j}\omega\phi\rho_0(\widetilde{\alpha} - \alpha_\infty), \tag{A2}$$

$\widetilde{\alpha}$ is the dynamic tortuosity defined by

$$\widetilde{\alpha} = 1 - \frac{\mathrm{j}\phi\sigma}{\alpha_\infty\rho_0\omega}\sqrt{1 - \frac{4\mathrm{j}\alpha_\infty^2\eta_a\rho_0\omega}{(\sigma\Lambda\phi)^2}}. \tag{A3}$$

$\sigma$ is the flow resistivity, $\eta_a$ is the dynamic viscosity of air and $\Lambda$ is the viscous characteristic length. The equivalent density $\widetilde{\rho}_{eq}$ and coupling coefficient are given by

$$\widetilde{\rho}_{eq} = \frac{\widetilde{\rho}_{22}}{\phi^2}, \quad \widetilde{\gamma} = \phi\left(\frac{\widetilde{\rho}_{12}}{\widetilde{\rho}_{22}} - \frac{1-\phi}{\phi}\right). \tag{A4}$$

The thermal properties are given by the dynamic compressibility $\widetilde{K}_{eq}$,

$$\widetilde{K}_{eq} = \frac{\gamma P_0}{\gamma - (\gamma-1)\left[1 + \dfrac{8\eta_a}{\mathrm{j}\Lambda' Pr\omega\rho_0}\sqrt{1 + \dfrac{\mathrm{j}\rho_0\omega Pr\Lambda'^2}{16\eta_a}}\right]^{-1}}, \tag{A5}$$

where $\Lambda'$ is the thermal characteristic length, $Pr$ is the Prandtl number, $P_0$ is the ambiant pressure, $\gamma$ is the ratio of specific heats of air. For sound absorbing materials, one has

$$\widetilde{Q} = \phi(1-\phi)\widetilde{K}_{eq}, \quad \widetilde{R} = \phi^2\widetilde{K}_{eq}. \tag{A6}$$

The structural mechanical parameters $N$ and $\hat{A}$ are given by

$$N = \frac{E(1+\mathrm{j}\eta_s)}{2(1+\nu)}, \quad \hat{A} = \frac{2N\nu}{1-2\nu}, \quad \hat{P} = \hat{A} + 2N. \tag{A7}$$

The two compressional waves of the porous medium are defined by their wave number $\delta_i$ and the ratio of the total displacement over the solid one $\mu_i$. They are defined by

$$\delta_i^2 = \frac{\left(\delta_{s2}^2 + \delta_{eq}^2\right) \pm \sqrt{\left(\delta_{s2}^2 + \delta_{eq}^2\right)^2 - 4\delta_{eq}^2\delta_{s1}^2}}{2}, \tag{A8}$$

with

$$\delta_{eq} = \omega\sqrt{\frac{\widetilde{\rho}_{eq}}{\widetilde{K}_{eq}}}, \quad \delta_{s1} = \omega\sqrt{\frac{\widetilde{\rho}}{\hat{P}}}, \quad \delta_{s2} = \omega\sqrt{\frac{\widetilde{\rho}_s}{\hat{P}}}, \tag{A9}$$

with

$$\widetilde{\rho} = \rho_1 - \widetilde{\rho}_{12} - \frac{\widetilde{\rho}_{12}^2}{\rho_2 - \widetilde{\rho}_{12}}, \quad \widetilde{\rho}_s = \widetilde{\rho} + \widetilde{\gamma}^2\widetilde{\rho}_{eq} \tag{A10}$$

and

$$\mu_i = \widetilde{\gamma}\frac{(\delta_i^2 - \delta_{s2}^2)}{\delta_{s2}^2 - \delta_{s1}^2} = \widetilde{\gamma}\frac{\delta_{eq}^2}{\delta_i^2 - \delta_{eq}^2}. \tag{A11}$$

## A2. Matrices for monodimensional problems

$$\left[\mathbf{K}_0\right] = \frac{1}{h}\begin{bmatrix} 1 & -1 & 0 & 0 & 0 \\ -1 & 2 & -1 & 0 & 0 \\ 0 & \ddots & \ddots & \ddots & 0 \\ 0 & \ddots & -1 & 2 & -1 \\ 0 & & 0 & -1 & 1 \end{bmatrix} \tag{A12}$$

$$\left[\mathbf{M}_0\right] = \frac{h}{6}\begin{bmatrix} 2 & 1 & 0 & 0 & 0 \\ 1 & 4 & 1 & 0 & 0 \\ 0 & \ddots & \ddots & \ddots & 0 \\ 0 & \ddots & 1 & 4 & 1 \\ 0 & & 0 & 1 & 2 \end{bmatrix} \tag{A13}$$

$$\left[\mathbf{K}_0'\right] = \frac{1}{h'}\begin{bmatrix} 1 & -1 & 0 & 0 & 0 \\ -1 & 2 & -1 & 0 & 0 \\ 0 & \ddots & \ddots & \ddots & 0 \\ 0 & \ddots & -1 & 2 & -1 \\ 0 & & 0 & -1 & 2 \end{bmatrix} \tag{A14}$$

$$\left[\mathbf{M}_0'\right] = \frac{h'}{6}\begin{bmatrix} 2 & 1 & 0 & 0 & 0 \\ 1 & 4 & 1 & 0 & 0 \\ 0 & \ddots & \ddots & \ddots & 0 \\ 0 & \ddots & 1 & 4 & 1 \\ 0 & & 0 & 1 & 4 \end{bmatrix} \tag{A15}$$

$h$ and $h'$ correspond to the length of the elements.

### References


[1] J. Allard: Propagation of sound in porous media. Modelling sound absorbing materials. New York and London, 1993.

[2] N. Dauchez, S. Sahraoui, N. Atalla: Investigation and modelling of damping in a plate with a bonded porous layer. Journal of Sound and Vibration **265** (2003) 437–449.

[3] O. Dazel, F. Sgard, F. Becot, N. Atalla: Expressions of dissipated powers and stored energies in poroelastic media modeled by [bold u],[bold U] and [bold u],P formulations. The Journal of the Acoustical Society of America **123** (2008) 2054–2063.

[4] M. Biot: Theory of propagation of elastic waves in a fluid-filled-saturated porous solid. Journal of the Acoustical Society of America **28** (1956) 168–191.

[5] D. Johnson, J. Koplik, R. Dashen: Theory of dynamic permeability and tortuosity in fluid-saturated porous media. Journal of Fluid Mechanics **176** (1987) 379–402.

[6] Y.Champoux, J. Allard: Dynamic tortuosity and bulk modulus in air-saturated porous media. Journal of Applied Physics **70** (1991) 1975–1979.

[7] Y.Kang, J. Bolton: Finite element modeling of isotropic porous materials coupled with acoustical finite elements. Journal of the Acoustical Society of America **98** (1995) 635–643.

[8] R. Panneton, N. Atalla, F.Charron: A finite-element formulation for the vibroacoustic behavior of double-plate structures with cavity absorption. Canadian aerospace journal **41** (1995) 5–12.

[9] R. Panneton, N. Atalla: An efficient finite element scheme for solving the three-dimensional poroelasticity problem in acoustics. Journal of the Acoustical Society of America **101** (1997) 3287–3298.

[10] P.Göransson: A 3D, symetric finite element formulation of the biot equations with application to acoustic wave propagation through an elastic porous medium. International Journal for Numerical Methods in Engineering **41** (1998) 167–192.

[11] N. Atalla, R. Panneton, P. Debergue: A mixed displacement-pressure formulation for poroelastic materials. Journal of the Acoustical Society of America **104** (1998) 1444–1452.

[12] N. Atalla, M. Hamdi, R. Panneton: Enhanced weak integral formulation for the mixed (u,p) poroelastic equations. Journal of the Acoustical Society of America **109** (2001) 3065–3068.

[13] O. Dazel, B. Brouard, N. Dauchez, A. Geslain: Enhanced Biot's finite element displacement formulation for porous materials and original resolution methods based on normal modes. Acta Acustica united with Acustica **95** (2009) 527–538.

[14] N. Hörlin, M. Nordström, P. Göransson: A 3D hierarchical FE formulation of Biot's equations for elasto-acoustic modelling of porous media. Journal of Sound and Vibration **243** (2001) 633–652.

[15] S. Rigobert, F.C. Sgard, N. Atalla: A two-field hybrid formulation for multilayers involving poroelastic, acoustic, and elastic materials. Journal of the Acoustical Soci-ety of America **115** (2004) 2786–2797. http://link.aip.org/link/?JAS/115/2786/1.

[16] N. Dauchez, S. Sahraoui, N. Atalla: Convergence of poroelastic finite elements based on biot displacement formulation. Journal of the Acoustical Society of America **109** (2001) 33–40.

[17] R. Craig Jr.: Structural dynamics: An introduction to computers methods. John Wiley and Sons, New York, 1981.

[18] R. Craig Jr.: A review of time-domain and frequency-domain component-mode synthesis methods. Journal of Modal Analysis **2** (1987) 59–72.

[19] W. Hurty: Dynamic analysis of structural systems using component modes. A.I.A.A. Journal **3** (1965) 678–685.

[20] R. Craig Jr.: Substructure coupling for dynamic analysis and testing. Technical Report CR 2781, NASA, 1977.

[21] M. Tournour, N. Atalla, O. Chiello, F. Sgard: Validation, performance, convergence and application of free interface components mode synthesis. Computers & Structures **79** (2001) 1861–1876.

[22] M. A. Tournour, N. Atalla: Pseudostatic corrections for the forced vibroacoustic response of a structure-cavity system. Journal of the Acoustical Society of America **107** (2000) 2379–2386.

[23] Nastran advanced dynamics analysis user's guide. MSC Software.

[24] O. Dazel, F. Sgard, C.-H. Lamarque, N. Atalla: An extension of complex modes for the resolution of finite-element poroelastic problems. Journal of Sound and Vibration **253** (2002) 421–445.

[25] O. Dazel, F. Sgard, C.-H. Lamarque: Application of generalized complex modes to the calculation of the forced response of three dimensional poroelastic materials. Journal of Sound and Vibration **268** (2003) 555–580.

[26] F.Sgard, N. Atalla, R. Panneton: A modal reduction technique for the finite element formulation of Biot's poroelasticity equations in acoustics applied to multilayered structures. 16th International Congress on Acoustics/135th meeting of the Acoustical Society of America, Seattle, WA, USA, 1998, 1183–1184.

[27] O. Dazel, B. Brouard, C. Depollier, S. Griffiths: An alternative Biot's displacement formulation for porous materials. Journal of the Acoustical Society of America **121** (2007) 3509–3516.